0090-9556/11/3906-1070–1078$25.00
DRUG METABOLISM AND DISPOSITION
Vol. 39, No. 6
37523/3690349
DMD 39:1070–1078, 2011
Printed in U.S.A.

Complex Drug Interactions of HIV Protease Inhibitors 1: Inactivation, Induction, and Inhibition of Cytochrome P450 3A by Ritonavir or Nelfinavir

Brian J. Kirby, Ann C. Collier, Evan D. Kharasch, Dale Whittington, Kenneth E. Thummel, and Jashvant D. Unadkat

Departments of Pharmaceutics (B.J.K., D.W., K.E.T., J.D.U.) and Medicine (A.C.C.), University of Washington, Seattle Washington; and Department of Anesthesiology, Washington University, St. Louis, Missouri (E.D.K.)

Received December 3, 2010; accepted March 9, 2011

ABSTRACT:

Conflicting drug-drug interaction (DDI) studies with the HIV protease inhibitors (PIs) suggest net induction or inhibition of intestinal or hepatic CYP3A. As part of a larger DDI study in healthy volunteers, we determined the effect of extended administration of two PIs, ritonavir (RTV) or nelfinavir (NFV), or the induction-positive control rifampin on intestinal and hepatic CYP3A activity as measured by midazolam (MDZ) disposition after a 14-day treatment with the PI in either staggered (MDZ ~12 h after PI) or simultaneous (MDZ and PI coadministered) manner. Oral and intravenous MDZ areas under the plasma concentration-time curves were significantly increased by RTV or NFV and were decreased by rifampin. Irrespective of method of administration, RTV decreased net intestinal and hepatic CYP3A activity, whereas NFV decreased hepatic but not intestinal CYP3A activity. The magnitude of these DDIs was more accurately predicted using PI CYP3A inactivation parameters generated in sandwich-cultured human hepatocytes rather than human liver microsomes.

Introduction

The clinical use of HIV protease inhibitors (PIs) is complicated by their profound drug-drug interactions (DDIs). These interactions primarily result from inactivation and inhibition of the cytochrome P450 enzymes CYP3A (Kumar et al., 1996; Koudriakova et al., 1998; Lillibridge et al., 1998; Ernest et al., 2005). Ritonavir (RTV) is almost exclusively used in combination with other PIs, for its ability to inactivate CYP3A and "pharmacologically boost" the bioavailability of other PIs (e.g., lopinavir and saquinavir) (Zeldin and Petruschke, 2004). However, PIs may produce unexpected DDIs or fail to interact with commonly used CYP3A substrate drugs when expected. For example, with acute dosing, RTV significantly decreases alprazolam (a CYP3A substrate) clearance (Greenblatt et al., 2000a). Yet, paradoxically, with chronic administration, RTV has no effect on alprazolam clearance (Norvir product labeling; Abbott Laboratories, Abbott Park, IL). In addition, although PIs are thought to be eliminated primarily by CYP3A metabolism, upon chronic administration, despite CYP3A inactivation, they induce their own clearance (Hsu et al., 1997; Bardsley-Elliot and Plosker, 2000). These findings have been attributed to net induction of CYP3A (Hsu et al., 1997; Bardsley-Elliot and Plosker, 2000; Greenblatt et al., 2000a). This is an unsatisfactory explanation based on human liver microsomes (HLMs) studies, in which PIs are potent inactivators of CYP3A and therefore are predicted to completely inactivate CYP3A in vivo (Koudriakova et al., 1998; Ernest et al., 2005). Moreover, such an explanation is at odds with interaction studies with other CYP3A substrates such as triazolam and zolpidem (Greenblatt et al., 2000b). Coadministration of these drugs results in profound interactions with PIs, even after extended administration, suggesting net inactivation of CYP3A activity. To complicate the DDI potential even further, many PIs induce other cytochromes P450 and P-glycoprotein in vitro in human hepatocytes (Dixit et al., 2007) and in vivo (Hughes et al., 2007) (Norvir product labeling).

The above factors make prediction of in vivo DDIs with PIs challenging from several points of view. First, is there net induction or inactivation of CYP3A activity (hepatic or intestinal) when PIs are administered chronically? Second, is net induction or inactivation of CYP3A activity dependent on staggered or simultaneous administration of the PI with the CYP3A drug? Third, can such complex interactions with PIs (including inactivation, induction, and inhibition) be quantitatively predicted from HLMs or sandwich-cultured human hepatocytes (SCHHs)? Fourth, are other enzymes and trans-

This work was supported by the National Institutes of Health National Institute of General Medical Sciences [Grant GM032165]; the National Institutes of Health National Institute on Drug Abuse [Grants K24-DA00417, R01-DA14211]; the National Institutes of Health National Center for Research Resources [Grant M01-RR-00037] (to the Clinical Research Center Facility at the University of Washington); the National Institutes of Health National Institute of General Medical Sciences [Grant GM07550] (Pharmacological Sciences Training; to B.J.K.); ARCS (to B.J.K.); and Simcyp (to B.J.K.).

Article, publication date, and citation information can be found at http://dmd.aspetjournals.org.

doi:10.1124/dmd.110.037523.

ABBREVIATIONS: PIs, anti-HIV protease inhibitors; DDI, drug-drug interaction; RTV, ritonavir; HLMs, human liver microsomes; SCHHs, sandwich-cultured human hepatocytes; NFV, nelfinavir; MDZ, midazolam; RIF, rifampin; OH, hydroxy; sWEM, supplemented Williams' E media; AUC, area under the plasma concentration-time curve; IS, internal standard; GI, gastrointestinal; GMR, geometric mean ratio.

porters induced by PIs and can the magnitude of such induction be predicted by SCHH experiments? Together, these complications lead to the question, Can the complex and paradoxical DDIs with the PIs be accurately predicted when multiple modes of interaction (inactivation, induction, and inhibition) are accounted for and more comprehensive in vitro tools (SCHHs) are used? To address this question, we conducted a series of in vivo and in vitro studies with RTV and nelfinavir (NFV) as prototypic PIs. In this article, we have addressed the first three points listed above; subsequent articles will address the fourth point.

In brief, we have determined whether there is net induction or inhibition of intestinal and hepatic CYP3A using intravenous and oral midazolam (MDZ) as the probe substrate after multiple doses (~14 days) of RTV (400 mg b.i.d.), NFV (1250 mg b.i.d.), or the induction-positive control rifampin (RIF) (600 mg q.d.) in the presence or absence of coadministration (staggered or simultaneous) of the PI or RIF. Then, using data on induction (Dixit et al., 2007; Fahmi et al., 2008b) of CYP3A protein and mRNA expression in human hepatocytes and inactivation of CYP3A in SCHHs or HLMs, we evaluated the ability of these in vitro models to accurately predict the magnitude of the CYP3A DDIs observed in our study. Because the PIs are capable of altering CYP3A activity by multiple mechanisms (inactivation, induction, and inhibition) and each mechanism is expected to alter CYP3A activity in vivo, it is important to include all three mechanisms in the prediction of in vivo interactions of the PIs with CYP3A enzymes. To do so, we used a modification (Kirby and Unadkat, 2010) of a comprehensive model that includes these three mechanisms (Fahmi et al., 2008b).

Materials and Methods

Subjects and Selection Criteria. All studies were approved by the University of Washington Institutional Review Board. Healthy volunteers (18–50 years) who provided written informed consent were enrolled in the study. Exclusion criteria included an abnormal EKG, fasting blood glucose of >110 mg/dl (study 1 only), a history of cardiac, hepatic, or renal disease, drug or alcohol abuse, HIV-positive status, chronic use of medications other than oral contraceptives, use of nonprescription medication that may interfere with the study, pregnancy or lactation, known allergies to study drugs, or smoking within 1 month of the study. Subjects were asked to avoid grapefruit-containing products, cruciferous vegetables, and herbal nutritional supplements for 3 weeks before and throughout the study and to avoid any acute medication, alcohol, caffeine, or dietary supplements for 24 h before and during each study session.

Study Design. This study is part of a larger study to evaluate the mechanisms of DDIs with NFV and RTV, consisting of two studies detailed in Fig. 1 and Table 1. The focus of this article is the CYP3A-mediated DDIs, and therefore we only address the effect of RTV, NFV, or RIF on intravenous and oral MDZ. In both studies, MDZ was given after ~14 days of treatment with RTV, NFV, or RIF. In study 1 (staggered administration), MDZ (either oral or intravenous) was given ~12 h after the last dose of RTV, NFV, or RIF. In study 2 (simultaneous administration), oral MDZ was given with a dose of RTV or NFV or 1 h after RIF. Study 1 was conducted in two arms (RTV and RIF treatment or NFV and RIF treatment). In study 2, all subjects were treated with RTV, NFV, and RIF. Order of treatment was randomized in all studies. Subjects fasted after midnight before each study session. In study 1 and study 2 (bupropion administration only), meals were held until 2 h after administration of the cocktails. In study 2, subjects were given a light standardized breakfast before cocktail A (in all sessions) to minimize gastrointestinal irritation by administration of RTV or NFV.

Study drugs were purchased from the following suppliers: midazolam (1 mg/ml syrup formulation; Boehringer Ingelheim, Ridgefield, CT), midazolam (1 mg/ml i.v. formulation; Ben Venue Laboratories, Inc., Bedford, OH), nelfinavir (625-mg tablets; Agouron Pharmaceuticals, Inc., La Jolla, CA), ritonavir (100-mg tablets; Abbott Laboratories, Abbott Park, IL), and rifampin (300-mg capsules; Sandoz, Broomfield, CO).

Chemicals and Reagents. MDZ, 1′-OH-MDZ, and stable labeled (D4) analogs [internal standard (IS) for MDZ and 1′OH-MDZ analysis] were purchased from Cerilliant Corporation (Round Rock, TX). Optima grade water, methanol, and methyl-*t*-butyl ether were purchased from Thermo Fisher Scientific (Waltham, MA). All other chemicals were reagent grade or higher.

Midazolam and Metabolite Assay. Concentrations of MDZ and 1′OH-MDZ from plasma and urine (after deconjugation with β-glucuronidase, urine only) were determined via ultra-performance tandem mass spectrometry (Premier XE mass spectrometer; Waters, Milford, CT) after either liquid/liquid extraction (100 μl of ammonium hydroxide and 4 ml of methyl-*t*-butyl ether) or precipitation with acetonitrile (2:1, v/v). Standards (calibration range of 0.1 to 100 ng/ml for both MDZ and 1′OH-MDZ; IS 10 ng/ml) and quality-control samples were prepared in a similar matrix and extracted or precipitated identically to the samples. Chromatographic separation was achieved on a

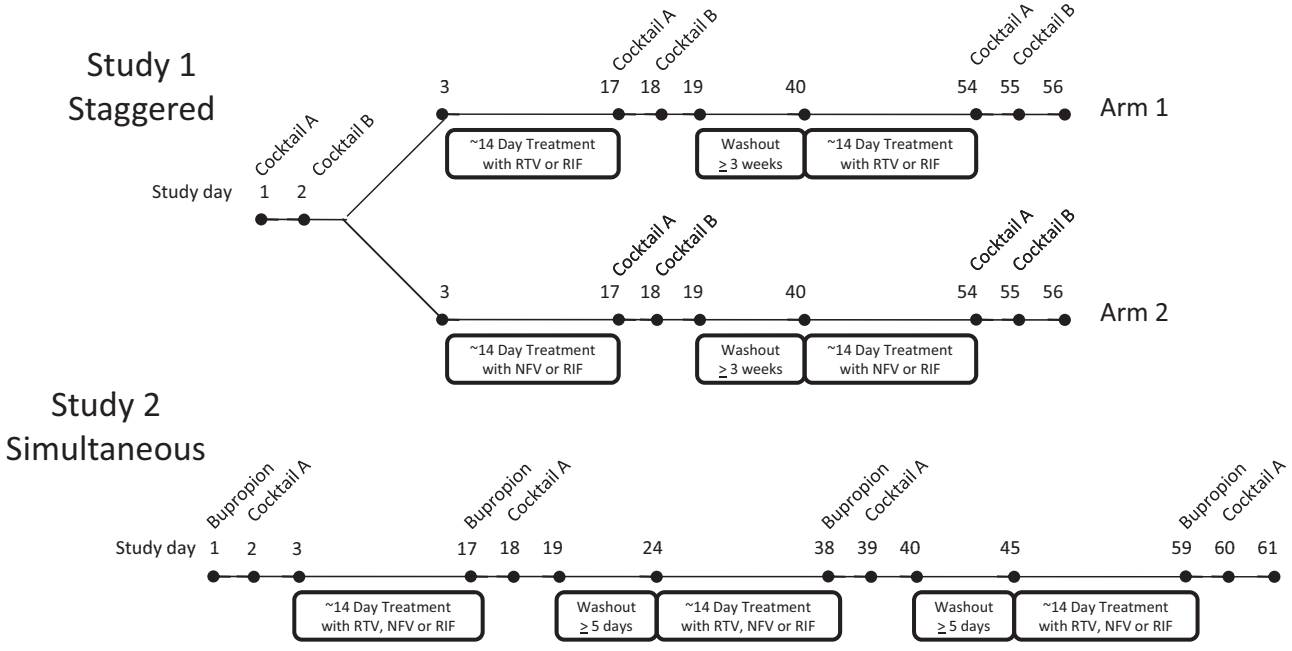

FIG. 1. Study design showing administration of probe drug cocktails before and after RTV, NFV, or RIF treatment. In study 1, the probe drug cocktails were staggered ~12 h after the last dose of RTV, NFV, or RIF. In study 2, a dose of RTV, NFV, or RIF was simultaneously administered with MDZ. For details on the components of cocktails, see Table 1.

TABLE 1

Subject characteristics and treatment period length

Subject Characteristics	Study 1: Staggered	Study 2: Simultaneous
Race		
Caucasian (Non-Hispanic/Latino)	14	9
Asian	1	0
Black/African American	1	0
Gender		
Male	5	3
Female	11	6
Age (years)		
Mean ± S.D.	33 ± 9	29 ± 9
Range	20–50	18–42
Weight (kg)		
Mean ± S.D.	78 ± 14	79 ± 14
Range	60–100	59–105
Treatment period days: average (minimum, maximum)		
Ritonavir (200 mg t.i.d. day 1, 300 mg b.i.d. days 2–7, 400 mg b.i.d. > day 8, dose escalation to minimize GI irritation)	14 (14, 15)	15 (15, 15)
Nelfinavir (1250 mg b.i.d.)	14 (13, 16)	14 (14, 15)
Rifampin (600 mg q.d.)	14 (12, 15)	15 (14, 15)
Probe drug administration		
Cocktail A	2 mg p.o. of midazolam at approximately 8:00 AM and 0.5 mg p.o. of digoxin at approximately 9:00 AM (24-h blood and urine collection)	
Cocktail B	1 mg i.v. of midazolam, 30 mg p.o. of dextromethorphan, 500 mg p.o. of tolbutamide, and 200 mg p.o. of caffeine at approximately 8:00 AM (24-h blood and urine collection)	
Bupropion	150 mg p.o. extended-release bupropion at approximately 8:00 AM (48-h blood and urine collection)	

UPLC BEH C18 2.1 × 50 mm 2-μm column (Waters), 0.3 ml/min flow rate with aqueous phase (0.1% acetic acid in water) and organic phase (0.1% acetic acid in methanol) and a rapid gradient from 95% aqueous to 100% organic over 2.5 min, using ion collection parameters (*m/z* transitions, cone voltages, and collision energy) for MDZ (326.0 < 291.2, 42, 27), D4 MDZ (330.0 < 295.2, 40, 27), 1′OH-MDZ (342.0 < 324.2, 35, 20), and D4 1′OH-MDZ (346.0 < 328.2, 40, 22), respectively.

Inactivation of CYP3A in SCHHS and HLMs. Inactivation parameters were calculated for RTV and NFV in HLMs (n = 3 livers) and SCHHs (n = 4 donors). HLM experiments were performed in duplicate at 37°C, with 0.25 mg/ml protein during the preincubation with RTV (0–1.0 μM, for 0, 0.5, 1, and 2 min) or NFV (0–5 μM, for 0, 1, 2, and 5 min), and then samples were diluted 1/10 before remaining CYP3A activity was measured by 1′OH-MDZ formation (20 μM MDZ, 3 min). Preincubation times were optimized to ensure adequate inactivation of CYP3A while minimizing depletion of RTV or NFV. Reactions were quenched with equal volumes of ice-cold methanol containing IS (50 ng/ml). Depletion of RTV or NFV during preincubation was monitored.

Freshly isolated human hepatocytes in a 96-well plate with Matrigel or Duragel overlay were purchased from CellzDirect (Durham, NC). After a 24-h equilibration period in serum-free supplemented Williams' E medium (sWEM; CellzDirect), cells were pretreated in duplicate with RTV (0–1 μM for 0, 1, 2.5, and 5 min) or NFV (0–5 μM for 0, 2.5, 5, and 10 min) in sWEM (≤1% methanol) at 37°C with 5% CO_2. Preincubation times were optimized to ensure adequate inactivation of CYP3A while minimizing depletion of RTV or NFV. After pretreatment, medium was removed (saved for depletion analysis), and cells were washed twice with phosphate-buffered saline containing 10% fetal bovine serum followed by one wash with phosphate-buffered saline. Then, sWEM containing midazolam (20 μM, ≤1% methanol) was incubated at 37°C with 5% CO_2 for 1 h, and the medium was removed and quenched with an equal volume of ice-cold methanol containing IS (50 ng/ml).

Relative quantification of 1′-OH-MDZ formation and depletion of RTV or NFV from HLM and SCHH experiments was performed by liquid chromatography-mass spectrometry using a Micromass platform LCZ mass spectrometer in positive electrospray mode with a Waters 2695 high-performance liquid chromatograph (Waters, Milford, MA) and gradient elution (0.1% acetic acid in water and methanol) on an XDB-C8 column (2.1 × 50 mm 5 μm; Agilent Technologies, Santa Clara, CA) with a C8 guard cartridge (Phenomenex, Torrance, CA). RTV or NFV concentrations were log average-adjusted if depletion was >10% by calculating the log-interpolated RTV or NFV area under the concentration-time curve (AUC) during the incubation period divided by the incubation time (log average concentration over the preincubation period).

Pharmacokinetic Analysis. Noncompartmental analysis of plasma concentration-time profiles of intravenous and oral MDZ was performed using WinNonlin Professional (version 5.0; Pharsight, Mountain View, CA). Parameters estimated included AUC, terminal plasma half-life ($t_{1/2}$), and oral or intravenous clearance (dose/$AUC_{0-\infty}$). Renal clearance (Cl_r) of MDZ was estimated by the ratio of the total amount of MDZ excreted in 24 h and MDZ AUC_{0-24}. Formation clearance of 1′-OH-MDZ was estimated by the ratio of the amount of 1′-OH-MDZ excreted (conjugated and unconjugated) in the 24-h urine and MDZ AUC_{0-24}. Residual MDZ from the oral administration was stripped from the intravenous administration profiles using the $t_{1/2}$ from intravenous administration and MDZ concentration before intravenous dosing. MDZ bioavailability (F) was determined by the ratio of oral and intravenous clearances. Hepatic bioavailability (F_H) and gastrointestinal bioavailability (F_G) were estimated, assuming negligible extrahepatic metabolism after intravenous administration, liver blood flow of 0.0216 l/min/kg, negligible partitioning of MDZ into red blood cells, hematocrit of 0.48, and the fraction of MDZ dose absorbed: F_{Abs} = 1.0 (Thummel et al., 1996). The fold change in hepatic CYP3A intrinsic clearance ($f_{Cl_{int}}^{Hep}$) upon treatment by RTV, NFV, or RIF was estimated using eq. 1, which is a rearrangement of an equation describing the predicted AUC ratio of an intravenously administered drug (Kirby and Unadkat, 2010). In eq. 1, $f_{m,\,CYP3A,\,Hep}$ is the fraction of hepatic clearance via CYP3A, EH is the hepatic extraction ratio of the probe drug before treatment, f_{hep} is the fraction of systemic clearance as a result of hepatic clearance, and $RAUC_{i.v.}$ is the ratio of AUC of the intravenously administered probe drug in the presence and absence of the DDI.

$$f_{Cl_{int}}^{Hep} = 1 + \frac{1}{f_{m,CYP3A,Hep}}\left[\frac{1}{\frac{1}{(1/EH-1)}\left[\frac{1/EH}{\frac{1}{f_{hep}}\left[\frac{1}{RAUC_{i.v.}}+f_{hep}-1\right]}-1\right]}-1\right] \quad (1)$$

The fold change in intestinal intrinsic clearance ($f_{Cl_{int}}^{GI}$) was calculated using the fold change in hepatic intrinsic clearance from eq. 1 and a rearrange-

ment of the model of Fahmi et al. (2008b) (eq. 2). In eq. 2, $RAUC_{p.o.}$ is the AUC ratio of the orally administered object drug in the presence and absence of the interaction.

$$f_{Cl_{int}}^{GI} = \frac{\frac{1}{RAUC_{i.v.}} * \frac{1}{f_{Cl_{int}}^{Hep} \times f_{m,CYP3A,Hep} + (1 - f_{m,CYP3A,Hep})} - F_G}{1 - F_G} \quad (2)$$

Statistical Analysis. A paired, two-tailed Student's *t* test was used to determine whether treatment significantly altered the pharmacokinetics of MDZ. Because pharmacokinetic parameters are typically log normally distributed, we also calculated the geometric mean ratio (GMR) by exponentiation of the average difference of log-transformed pharmacokinetic parameters. If the 90% confidence interval of the GMR included 1.0, the treatment was considered to not have significantly altered the pharmacokinetic parameter.

Using historical data for MDZ in healthy volunteers (Wang et al., 2001; Kirby et al., 2006), we conducted an a priori power analysis using the AUC of MDZ as the primary outcome measure. Assuming equal variance between control and treatment groups, our analysis indicated that $n = 7$ would provide 80% power ($\alpha < 0.05$) to discern 54 and 41% changes in oral and intravenous MDZ AUC, respectively.

In Vitro to In Vivo Prediction. The observed AUC ratios for intravenous (eq. 3) and oral (eq. 4) MDZ were predicted using in vitro CYP3A inactivation, induction, and inhibition parameters of the PIs generated in HLMs and SCHHs (Tables 2 and 3) and the two steady-state models (Fahmi et al., 2008b; Kirby and Unadkat, 2010):

$$\frac{AUC_{i.v.}^{'}}{AUC_{i.v.}} = \frac{1}{f_{hep}\left(\frac{1/EH}{\left(\left(\frac{1}{EH} - 1\right)\left(\frac{1}{(f_{m,CYP3A,Hep} \times f_{Cl_{int}}^{Hep}) + (1 - f_{m,CYP3A,Hep})}\right) + 1\right)}\right) + (1 - f_{hep})} \quad (3)$$

$$\frac{AUC_{p.o.}^{'}}{AUC_{p.o.}} = \frac{1}{f_{Cl_{int}}^{Hep} \times f_{m,CYP3A,Hep} + (1 - f_{m,CYP3A,Hep})} * \frac{1}{f_{Cl_{int}}^{GI} \times (1 - F_G) + F_G} \quad (4)$$

For simultaneous administration (study 2), $f_{Cl_{int}}^{Hep}$ was calculated using unbound average concentrations ($C_{ave,u}$) of RTV, NFV, or RIF as the driving force for inhibition, induction, and inactivation with a 36-h CYP3A degradation half-life following eq. 4, and $f_{Cl_{int}}^{GI}$ was calculated using the predicted unbound maximum enterocyte concentration (Obach et al., 2007) and a CYP3A degradation half-life of 24 h following the model of Fahmi et al. (2008b). Parameters (E_{max} and EC_{50}) describing induction of CYP3A protein or mRNA were estimated from our previously published studies in human hepatocytes (Dixit et al., 2007). Because our in vivo MDZ induction data after RIF treatment did not allow for estimation of induction of CYP3A (hepatic extraction exceeding hepatic plasma flow), induction of another CYP3A probe drug (alfentanil) after a similar RIF treatment regimen (Kharasch et al., 2004) was used as an in vitro to in vivo calibrator for CYP3A induction by estimating a scaling factor similar to the "d" value used by Fahmi et al. (2008b). The factor that allowed for adequate prediction of the AUC ratio (0.38) of alfentanil

TABLE 2

Midazolam parameters used for AUC ratio predictions

	Parameter
EH	0.57
f_{Hep}	0.994
$f_{m,\ CYP3A,\ Hep}$	0.92
F_G	0.78
F_G' (study 1: staggered)	0.92

TABLE 3

Precipitant parameters used for midazolam AUC ratio predictions

	Dose	C_{ave}	f_u	CYP3A Inhibition: $K_{i,\ CYP3A}$	CYP3A Inactivation						CYP3A Induction[b]				
					HLMs ($n = 3$)[a]			SCHHs Slope ($n = 4$)[a]	HLMs/SCHHs Slope	Protein[b]		mRNA Expression[b]			
					K_I	k_{inact}	k_{inact}/K_I[c]			$EC_{50,\ CYP3A}$	E_{max}	$EC_{50,\ CYP3A}$	E_{max}		
		μM		*μM*	*μM*	*min*$^{-1}$	*μM*$^{-1}$ · *min*$^{-1}$	*μM*$^{-1}$ · *min*$^{-1}$		*μM*	*fold*	*μM*	*fold*		
RTV	400 mg b.i.d.	8	0.015	0.25	0.25 (102)	0.33 (21)	2.31 (71)	0.174 (22)	13.3	3.4	13.9	23.8	67.9		
NFV	1250 mg b.i.d.	4	0.015	1.8	1.82 (70)	0.16 (36)	0.14 (80)	0.038 (67)	3.7	6.5	11.2	3.4	17.2		
RIF	600 mg q.d.	2	0.2	18.5	N.A.	N.A.	N.A.	N.A.	N.A.	9.7	21.9	16.3	62.6		

f_u, unbound fraction in plasma; $K_{i,\ CYP3A}$, reversible CYP3A inhibition constant; $EC_{50,\ CYP3A}$, concentration that results in half-maximal CYP3A protein or mRNA induction; E_{max}, maximum fold induction of CYP3A protein or mRNA; N.A., not applicable.

[a] Data are average values (% coefficient of variation).

[b] Estimated from Dixit et al. 2007.

[c] Reported value is the average (% coefficient of variation) of k_{inact}/K_I estimated for each HLM.

after RIF treatment (assuming $f_{m,\,CYP3A,\,Hep} = 0.98$ and EH = 0.28 using eq. 1) was used to scale in vivo induction of CYP3A predicted from hepatocytes (Tables 2 and 3).

In study 1, MDZ was administered ~12 h after a dose of RIF, RTV, or NFV. Therefore, the driving force concentration for estimating $f_{Cl_{int}}^{Hep}$ for CYP3A inhibition was unbound trough concentration ($C_{min,\,u}$), but $C_{ave,\,u}$ was used for inactivation and induction. Because of the staggered administration of MDZ and RTV or NFV, the estimation of $f_{Cl_{int}}^{GI}$ using eq. 4 is not acceptable. Therefore, we assumed that intestinal CYP3A was completely abolished as a result of potent inactivation, and the recovery of intestinal CYP3A was predicted on the basis of the 24-h degradation half-life of CYP3A (governed by enterocyte turnover) (Greenblatt et al., 2003; Culm-Merdek et al., 2006). On the basis of these assumptions, intestinal CYP3A activity would recover by ~30% after 12 h, which equates to a MDZ F_G' of 0.92. Therefore, the oral MDZ AUC ratio in study 1 was predicted using eq. 5 in which F_G' was set at 0.92:

$$\frac{AUC_{p.o.}^{'}}{AUC_{p.o.}} = \frac{1}{f_{Cl_{int}}^{Hep} \times f_{m,CYP3A} + (1 - f_{m,CYP3A})} \cdot \frac{F_G^{'}}{F_G} \quad (5)$$

Results

Seven subjects (healthy volunteers; Table 1) completed each arm of study 1 (staggered administration of the PIs and MDZ) and 9 subjects (except for NFV, $n = 8$) completed study 2 (simultaneous administration of the PIs and MDZ).

Midazolam Pharmacokinetics. NFV and RTV significantly increased the AUC and decreased the systemic and oral clearance of intravenous and oral MDZ administered in a staggered or simultaneous manner (Fig. 2; Table 4). As expected, RIF significantly increased oral and intravenous clearances of MDZ in both studies. intravenous blood clearance of MDZ after RIF treatment was increased to 2.0 l/min, which exceeds hepatic blood flow (1.5 l/min), implying extrahepatic clearance of MDZ, probably intestinal. Midazolam oral clearances and AUC GMRs were not statistically different for staggered (study 1) versus simultaneous administration (study 2) for all three treatments (RTV, NFV, and RIF). The only statistically significant difference between staggered and simultaneous administration was 1′-OH-MDZ oral formation clearance (oral $Cl_{formation}$) after treatment with RTV; simultaneous administration showed a greater decrease than staggered administration. Because of the study design (Fig. 1), it was possible to evaluate the bioavailability ($F_A \cdot F_G$, F_H, and F) of MDZ only with staggered administration. The oral bioavailability (F) of MDZ was significantly increased by RTV and decreased by RIF. In contrast, NFV treatment did not significantly change F of MDZ, probably because of a greatly variable effect in the intestine. F_G was significantly increased by RTV but not statistically increased by NFV. F_H was significantly increased by NFV or RTV. Thus, RTV significantly decreased both hepatic and intestinal CYP3A activity ($f_{Cl_{int}}^{Hep}$ and $f_{Cl_{int}}^{GI}$ respectively), whereas NFV significantly decreased only hepatic CYP3A activity ($f_{Cl_{int}}^{Hep}$) (Table 4). Because of the apparent extrahepatic metabolism of MDZ after RIF treatment, estimates of F_H, F_G, $f_{Cl_{int}}^{Hep}$, or $f_{Cl_{int}}^{GI}$ were not possible.

CYP3A Inactivation in SCHHs and HLMs. Inactivation of CYP3A by RTV or NFV in HLMs and SCHHs showed concentration and time dependence (Fig. 3, A–D). In contrast to HLMs, in SCHHs, a hyperbolic plot of λ (observed inactivation rate constant) versus inactivator concentration was not consistently observed up to concentrations of 1 μM for RTV or 5 μM for NFV (Fig. 3, E and F, respectively). Therefore, the average slope of the linear portion of this curve was determined (0.174 ± 0.037 and 0.038 ± 0.026 μM^{-1} min^{-1} for RTV and NFV, respectively). The average slopes of λ versus inactivator concentration in SCHHs are 13- and 3.7-fold lower (RTV and NFV, respectively) than the initial slopes (k_{inact}/K_I) in HLMs (Table 3). The individual and average slopes in SCHHs ($n = 4$) for RTV and NFV up to 1 μM were compared with the average hyperbolic profiles in HLMs (Fig. 3, G and H). Use of the slope of λ versus inactivator concentration for in vivo prediction is applicable because the unbound average RTV or NFV plasma concentrations are within the linear region of the plots (<1 μM).

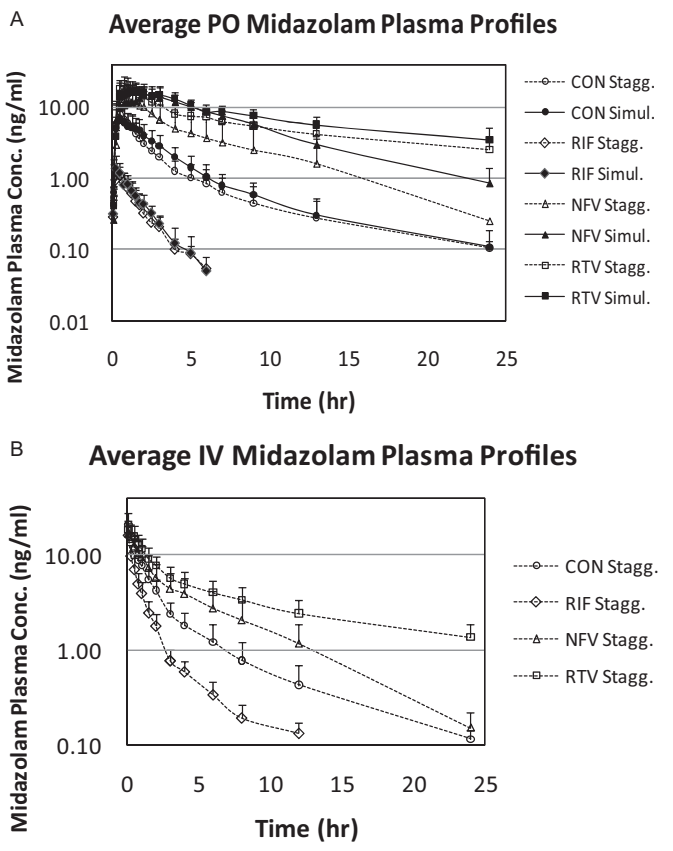

FIG. 2. Mean (±S.D.) plasma concentration-time profiles of oral (A) and intravenous (B) MDZ before (CON) or after treatment with RTV, NFV, or RIF. In study 1 (dashed lines and open symbols) MDZ administration was staggered (Stagg.) ~12 h after the last dose of RTV, NFV, or RIF, whereas in study 2 (solid lines and closed symbols) MDZ was simultaneously administered (Simul.) with a dose of RTV, NFV, or RIF.

In Vitro to In Vivo Prediction. The in vitro to in vivo scaling factors for induction of CYP3A estimated from the RIF interaction with alfentanil (Kharasch et al., 2004) were 9.6 and 5.5 using protein and mRNA expression, respectively. The predicted AUC ratios for the DDIs between MDZ and RTV or NFV using HLM- or SCHH-derived inactivation parameters and protein or mRNA expression for induction were compared with those observed (Fig. 4A). In general, the HLM inactivation parameters overpredicted the interactions (greater than the 90% CI) irrespective of whether CYP3A protein or mRNA data were used for induction. In contrast, the SCHH inactivation parameters more accurately predicted the MDZ AUC ratios when either CYP3A protein or mRNA expression data were used for induction. The difference between the HLM- and SCHH-derived inactivation parameters was also apparent when the predictability of the fold change in hepatic CYP3A activity as a result of RTV or NFV treatment was evaluated (Fig. 4B). When protein expression was used to predict induction, in conjunction with the SCHH-derived inactivation parameters, the effect of RTV or NFV was accurately predicted. In contrast, when CYP3A4 mRNA expression was used for induction in conjunction with SCHH-derived inactivation parameters, the effect of RTV on hepatic CYP3A was overpredicted (a greater decrease in

TABLE 4

MDZ pharmacokinetic parameters before and after treatment with NFV, RTV, or RIF

Bold values are significantly different from control ($P < 0.05$, paired t test) or the 90% CI does not include unity.

	Control	Nelfinavir		Ritonavir		Rifampin	
		Avg. ± S.D.	GMR (90% CI)	Avg. ± S.D.	GMR (90% CI)	Avg. ± S.D.	GMR (90% CI)
Study 2: midazolam simultaneously administered with NFV, RTV, or RIF							
Oral							
$AUC_{0-\infty}$ (h · ng/ml)	25.7 ± 10.4	**136 ± 33**	**5.8 (4.5–7.5)**	**266 ± 99**	**10.5 (8.7–12.7)**	**2.49 ± 0.74**	**0.10 (0.08–0.13)**
Cl_{oral} (l/min)	1.51 ± 0.6	**0.26 ± 0.05**	**0.17 (0.13–0.22)**	**0.14 ± 0.05**	**0.10 (0.08–0.12)**	**14.5 ± 4.1**	**10.0 (7.7–12.9)**
Cl_{oral} (ml · min^{-1} · kg^{-1})	19.5 ± 8.3	**3.36 ± 0.86**	**0.17 (0.13–0.22)**	**1.85 ± 0.70**	**0.10 (0.08–0.12)**	**185 ± 51.3**	**10.0 (7.7–12.9)**
$Cl_{formation}$ (l/min)	1.10 ± 0.5	**0.12 ± 0.04**	**0.11 (0.08–0.15)**	**0.05 ± 0.02**	**0.05 (0.04–0.06)**	**9.2 ± 2.9**	**8.8 (6.7–11.4)**
$t_{1/2}$ (h)	4.7 ± 1.8	5.5 ± 2.5	**1.2 (1.03–1.5)**	**14 ± 7.7**	**2.9 (2.5–3.4)**	**1.5 ± 0.6**	**0.33 (0.27–0.41)**
Study 1: midazolam staggered administered with NFV, RTV, or RIF							
Oral							
$AUC_{0-\infty}$ (h · ng/ml)	22.7 ± 9.4	**77.4 ± 51.5**	**3.3 (1.9–5.5)**	**188 ± 33.0**	**8.4 (6.8–10.4)**	**1.84 ± 0.67**	**0.09 (0.07–0.11)**
Cl_{oral} (l/min)	1.73 ± 0.7	**0.62 ± 0.38**	**0.31 (0.18–0.52)**	**0.18 ± 0.04**	**0.12 (0.10–0.15)**	**20.3 ± 7.1**	**11.7 (9.3–14.8)**
Cl_{oral} (ml · min^{-1} · kg^{-1})	24.7 ± 11.5	**8.41 ± 6.44**	**0.31 (0.18–0.52)**	**2.43 ± 0.55**	**0.12 (0.10–0.15)**	**265 ± 94.4**	**11.7 (9.3–14.8)**
$Cl_{formation}$ (l/min)	1.14 ± 0.5	**0.40 ± 0.27**	**0.27 (0.15–0.50)**	**0.10 ± 0.05**	**0.10 (0.07–0.14)**	**9.8 ± 3.8**	**8.3 (6.4–10.8)**
$t_{1/2}$ (h)	3.8 ± 1.5	4.4 ± 1.5	1.1 (0.90–1.4)	**11.4 ± 3.8**	**3.2 (2.6–3.9)**	**0.97 ± 0.30**	**0.27 (0.22–0.32)**
Intravenous							
$AUC_{0-\infty}$ (h · ng/ml)	36.2 ± 10.4	**66.3 ± 22.0**	**2.0 (1.7–2.4)**	**120 ± 23.6**	**3.0 (2.7–3.4)**	**16.1 ± 2.9**	**0.48 (0.43–0.54)**
$Cl_{i.v.}$ (l/min)	0.49 ± 0.11	**0.28 ± 0.09**	**0.51 (0.42–0.61)**	**0.14 ± 0.03**	**0.33 (0.30–0.37)**	**1.06 ± 0.17**	**2.1 (1.8–2.3)**
$Cl_{i.v.}$ (ml · min^{-1} · kg^{-1})	6.68 ± 1.62	**3.51 ± 1.17**	**0.51 (0.42–0.61)**	**1.92 ± 0.56**	**0.33 (0.30–0.37)**	**13.9 ± 2.32**	**2.1 (1.8–2.3)**
$Cl_{formation}$ (l/min)	0.34 ± 0.08	**0.16 ± 0.08**	**0.41 (0.29–0.56)**	**0.05 ± 0.02**	**0.19 (0.16–0.22)**	**0.68 ± 0.10**	**1.9 (1.7–2.1)**
$t_{1/2}$ (h)	4.1 ± 1.5	5.8 ± 4.2	1.2 (0.89–1.7)	**11.7 ± 6.3**	**2.7 (2.5–3.0)**	**2.5 ± 1.1**	**0.65 (0.57–0.73)**
F	0.31 ± 0.09	0.61 ± 0.24	1.7 (0.97–2.9)	**0.79 ± 0.13**	**2.8 (2.3–3.3)**	**0.06 ± 0.02**	**0.18 (0.15–0.23)**
F_H	0.43 ± 0.15	**0.69 ± 0.10**	**1.8 (1.5–2.1)**	**0.83 ± 0.05**	**1.8 (1.5–2.2)**		**N.A.**[a]
$F_A \cdot F_G$	0.78 ± 0.25	0.89 ± 0.37	0.96 (0.60–1.5)	**0.96 ± 0.20**	**1.5 (1.4–1.7)**		**N.A.**
Hepatic Cl_{int} fold change ($f_{Cl_{int}}^{Hep}$)		**0.24 ± 0.11**	**0.21 (0.13–0.34)**	**0.12 ± 0.09**	**0.10 (0.06–0.17)**		**N.A.**
GI Cl_{int} fold change ($f_{Cl_{int}}^{GI}$)		0.38 ± 1.4	0.55 (0.07–6.8)	−0.04 ± 0.45	**0.22 (0.10–0.48)**		**N.A.**

[a] N.A., not available. F_H, $F_A \cdot F_G$, $f_{Cl_{int}}^{GI}$, and $f_{Cl_{int}}^{Hep}$ are not available for MDZ after RIF treatment because of intravenous blood clearance exceeding the estimated hepatic blood flow. All reported clearance values are plasma clearances.

hepatic CYP3A than observed), but the effect of NFV was adequately predicted. Figure 4C validates our assumption that intestinal CYP3A activity can be predicted assuming complete inactivation of CYP3A activity after RTV or NFV dosing and estimating the intestinal recovery based on enterocyte half-life.

Discussion

Because of the unpredictable nature of CYP3A-mediated DDIs with the PIs, we conducted two studies to investigate the effect of RTV and NFV on intestinal and hepatic CYP3A activity in healthy volunteers. One study was designed to measure only the net effect of inactivation and induction of CYP3A and deliberately avoid acute inhibition of CYP3A produced by concomitant administration of the PIs and MDZ, whereas the second study was designed to evaluate the net effect, including inhibition of CYP3A. As a result of this study design we were able to determine whether net induction of CYP3A could occur in the liver or the intestine, which has been alluded to as an explanation for paradoxical DDIs with the PIs.

As we hypothesized, chronic administration of RTV did not result in net induction of intestinal or hepatic CYP3A activity. In fact, RTV treatment decreased intestinal CYP3A activity by ~78% ($f_{Cl_{int}}^{GI}$ = 0.22, 90% CI of 0.10–0.48) (Table 4), consistent with that expected on the basis of normal intestinal enzyme recovery over the 12-h dosing interval. RTV is known to activate PXR, thereby inducing transcription of CYP3A and other genes (Gupta et al., 2008). If synthesis of CYP3A was induced as little as 3-fold, recovery of ~90% of baseline CYP3A activity would be expected ($f_{Cl_{int}}^{GI}$ of 0.9). This result implies that either intestinal induction is minimal to nonexistent or systemic exposure of RTV is capable of inactivating intestinal CYP3A. The effect of NFV on $f_{Cl_{int}}^{GI}$ was more variable than that of RTV; two of the seven subjects showed no decrease or a net increase in $f_{Cl_{int}}^{GI}$ with a GMR of 0.55 (90% CI of 0.07–6.8, not statistically significant). In contrast to RTV, the average recovery of CYP3A activity is slightly greater than expected on the basis of intestinal enterocyte recovery half-life and time after NFV dosing, although this average is heavily influenced by two subjects showing no change or an increase in intestinal CYP3A. NFV, like RTV, is also known to activate PXR and induce CYP3A transcription (Gupta et al., 2008). This observation implies that either inactivation of CYP3A in the intestine may be incomplete or there is moderate and variable induction of intestinal CYP3A by NFV. The two subjects who showed no decrease or a net increase in intestinal CYP3A appear to have had adequate systemic exposure of NFV ($f_{Cl_{int}}^{Hep}$ = 0.27 and 0.33), implying compliance with NFV dosing. Therefore, we speculate that these two subjects may have either had much greater intestinal induction or lower exposure of the intestinal enterocytes by systemic NFV or during the absorption process.

Staggered administration of RTV or NFV substantially decreased $f_{Cl_{int}}^{Hep}$ in a less variable way than $f_{Cl_{int}}^{GI}$ with GMRs of 0.10 (90% CI of 0.06–0.17) and 0.21 (90% CI of 0.13–0.34), respectively (Table 4). Because MDZ was not administered intravenously in the simultaneous administration study, it was not possible to determine whether simultaneous administration of RTV or NFV resulted in a greater degree of hepatic or intestinal CYP3A inhibition. 1′-OH-MDZ formation clearance was affected to a greater extent by simultaneous administration of both NFV and RTV. This finding implies that the DDI is not mediated solely by CYP3A inactivation, but that there is a small contribution of reversible inhibition of CYP3A in the intestine and/or liver. This difference between staggered and simultaneous administration was not observed in oral clearance, probably because $f_{m,\,CYP3A}$ is less than 1.0, making formation clearance a more sensitive measure of CYP3A activity.

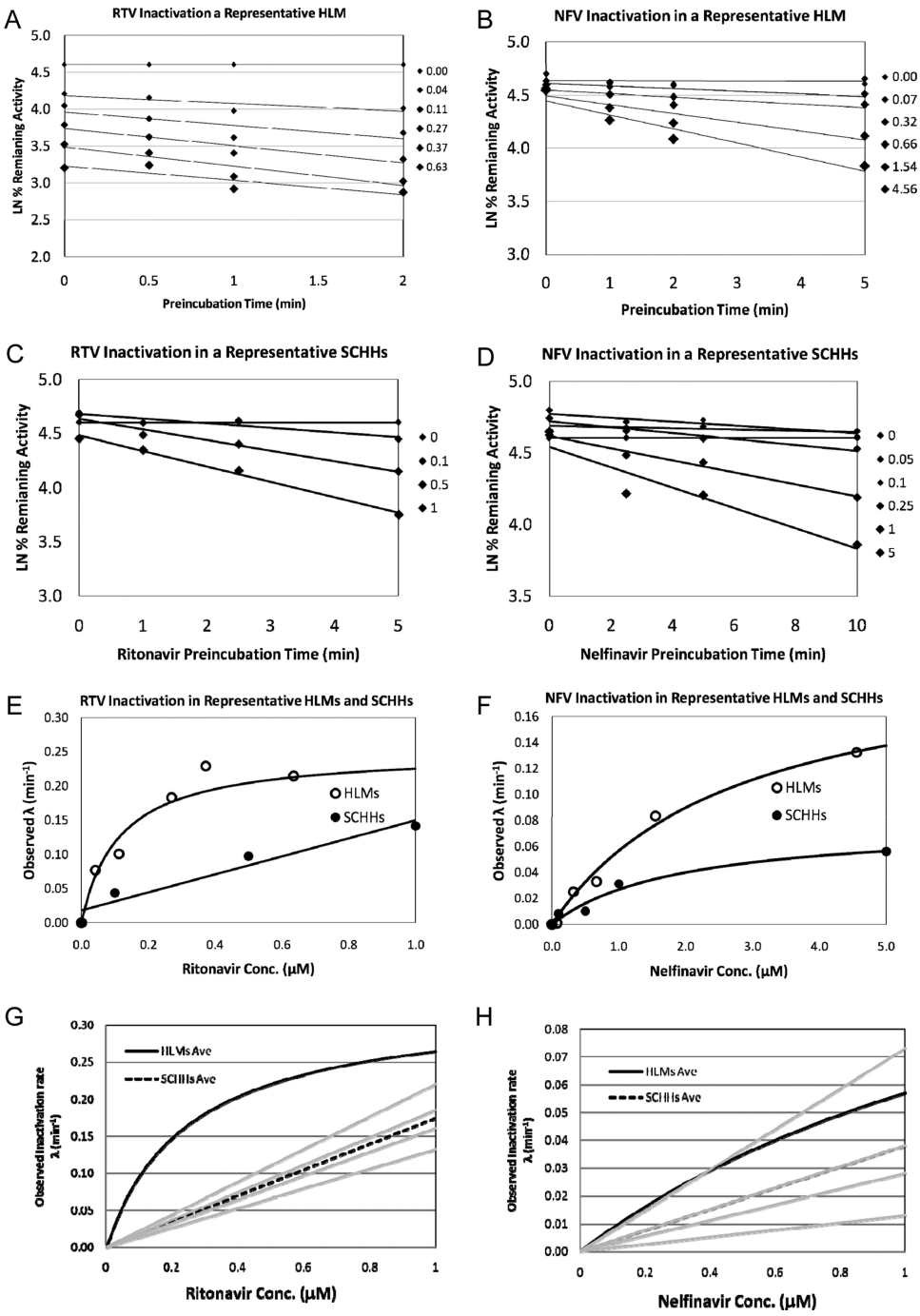

FIG. 3. CYP3A inactivation by RTV or NFV in HLMs versus SCHHs. Natural log (LN) percentage remaining CYP3A activity after RTV (A and C) or NFV (B and D) pretreatment measured in representative HLM and SCHH lots (micromolar concentrations of the inactivator are listed at the right of each panel). A combined plot of observed inactivation rate (λ, minute^{-1}) of CYP3A by RTV (E) or NFV (F) in representative HLM and SCHH lots. A combined plot of the linear fit of λ (minute^{-1}) of CYP3A by RTV (G) or NFV (H) in four different SCHHs (gray lines) and average linear fit (dashed line) compared with the average hyperbolic plot measured in HLMs ($n = 3$).

To quantitatively predict DDIs with RTV or NFV, all three mechanisms of their interaction with CYP3A (inactivation, inhibition, and induction) must be included in the predictive model. We used RIF as an in vitro to in vivo calibrator to quantitatively predict the in vivo fold induction of CYP3A activity by the PIs on the basis of human hepatocyte studies using protein and mRNA expression. These correction factors were 9.6 and 5.5, implying that induction of CYP3A observed in vivo is ~6- to 10-fold higher than that observed in hepatocytes. There are many possible reasons for this in vitro to in vivo discrepancy, including insensitivity of hepatocytes to induction compared with in vivo and different in vitro versus in vivo exposure profiles to the PIs. These and other in vitro to in vivo extrapolation issues have begun to be addressed (Ripp et al., 2006; Fahmi et al., 2008a, 2009; Almond et al., 2009) and will be addressed further in our next article. Using RTV and NFV in vitro inhibition and inactivation parameters of CYP3A measured in HLMs, we overpredicted our observed MDZ AUC ratios. This result implies that in vitro HLM data predict more potent net inhibition of CYP3A activity than is observed in vivo. Therefore, we asked whether SCHHs would better predict CYP3A inactivation in vivo with the PIs. Indeed, we found that inactivation of CYP3A in SCHHs is 13- and 4-fold lower for RTV and NFV, respectively, compared with that for HLMs. These differences may be even greater as a result of correcting for unbound fraction in HLMs ($f_{u,\,mic}$), which could be as high as 0.5 for RTV (Tran et al., 2002). Moreover, the SCHH-derived inactivation parameters more accurately predicted the observed DDIs with MDZ (Fig. 4). The mechanistic basis for the difference in CYP3A inactivation between HLMs and SCHHs is unknown, but we speculate that it may include

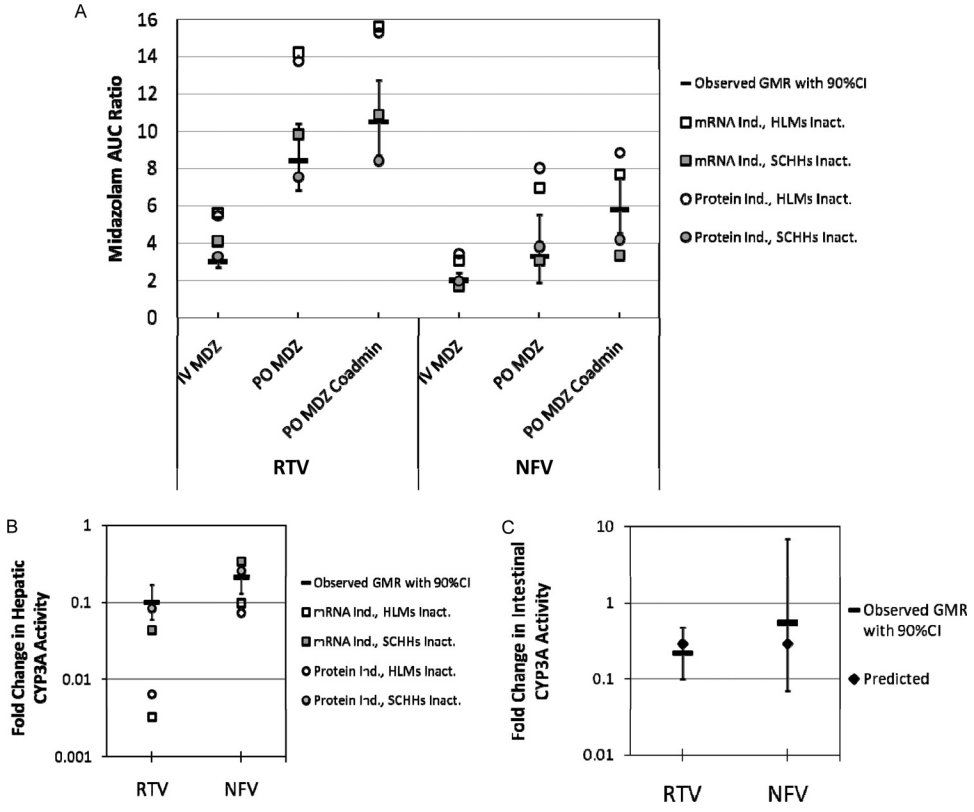

FIG. 4. The observed (GMR ± 90% CI) MDZ AUC ratios (A) (black bars with error bars) or fold change in hepatic CYP3A activity (B) caused by RTV or NFV were more accurately predicted using CYP3A4 mRNA expression (circles) or CYP3A protein (squares) for induction with inactivation parameters of CYP3A by RTV or NFV derived from SCHHs (closed symbols) compared with HLMs (open symbols). Observed (GMR ± 90% CI) intestinal CYP3A recovery (black bars with error bars) was accurately predicted by intestinal CYP3A recovery based on intestinal turnover (C).

canalicular efflux of RTV or NFV, intracellular metabolic depletion of the PIs, or other "protective" metabolic pathways present in SCHHs that are not present in HLMs. Such processes could lower the intracellular to extracellular concentration of the PI or the exposure of CYP3A to the inactivating species and thus decrease the inactivation potency of the PIs. The differing magnitude of CYP3A inactivation between HLMs and SCHHs is drug-specific, suggesting that it is not purely a system difference but is dependent on the inactivator tested. This may be a result of varying contributions of the three points listed above for each inactivator. These observations are consistent with those of Zhao (2008), who showed differing inactivation potency (time-dependent inactivation IC_{50}) between HLMs and suspended human hepatocytes for amprenavir and erythromycin but not for diltiazem, raloxifene, or troleandomycin. This finding highlights the importance of using SCHHs to determine CYP3A inactivation because this model includes the canalicular efflux processes that may determine intracellular drug concentrations. HLMs have historically provided adequate prediction of in vivo DDIs for many drugs, but as highlighted here with the PIs, RTV and NFV, this simplified system (HLMs) does not always mimic the complex system of the in vivo hepatocyte, and a more comprehensive in vitro model (SCHHs) could provide a better predictive tool for the in vivo situation. These results suggest the importance of determining the mechanistic basis for the difference in potency of inactivation between HLMs and SCHHs. Such studies could provide guidelines as to when it is necessary to use SCHHs versus HLMs for accurate in vivo predictions of DDIs.

In summary, we have shown that multiple-dose treatment of RTV results in a net decrease in hepatic and intestinal CYP3A activity irrespective of simultaneous or staggered RTV administration with the CYP3A victim drug. Thus, some other unknown mechanism(s) must be at play in the paradoxical DDIs with RTV such as alprazolam and autoinduction of the PIs. In addition, we have shown that CYP3A DDIs by the PIs are better predicted if inactivation parameters are derived from SCHHs. Our results also have clinical ramifications. In this study, we used a higher dose of RTV (400 mg versus 100 mg) for two reasons. First, this study was begun when this higher dose was more widely used, and second, some of the paradoxical DDIs and autoinduction were observed at this higher dose. Nevertheless, our results are also applicable at the lower dose of 100 mg. Others have shown profound increases in the AUC of MDZ (28-fold) (Greenblatt et al., 2009) and triazolam (40-fold) (Culm-Merdek et al., 2006) after short-term treatment (2 days) and a 20-fold increase in triazolam AUC after extended treatment (10 days) with low-dose RTV (100 mg b.i.d.). Therefore, we predict that RTV, even at the lower dose (100 mg b.i.d.) (Fig. 5), will result in net inactivation of hepatic CYP3A activity irrespective of whether it is administered simultaneously or

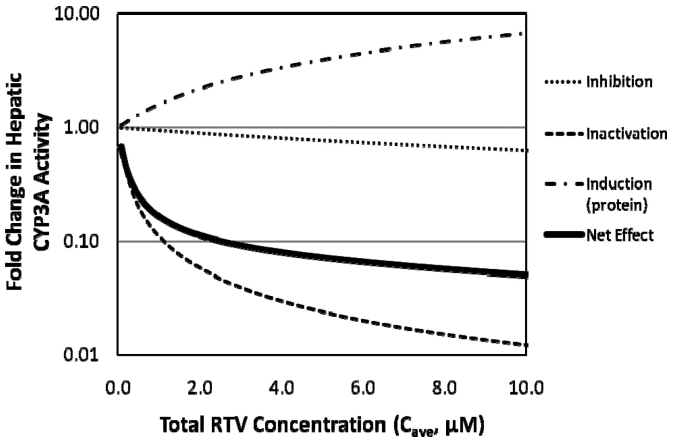

FIG. 5. The predicted contribution of inhibition, inactivation, and induction of hepatic CYP3A by RTV is shown across an applicable RTV total plasma concentration range, indicating that even at a low dose of RTV (100 mg b.i.d., ~1 μM) net hepatic CYP3A inactivation is predicted.

staggered with a CYP3A victim drug. The use of dynamic or physiologically based pharmacokinetic models may provide further insight into the intestinal and hepatic first-pass contribution to this prediction.

Acknowledgments

We thank Eric Helgeson and Christine Hoffer for clinical study coordination.

Authorship Contributions

Participated in research design: Kirby, Collier, Kharasch, Thummel, and Unadkat.

Conducted experiments: Kirby and Whittington.

Contributed new reagents or analytic tools: Whittington.

Performed data analysis: Kirby and Whittington.

Wrote or contributed to the writing of the manuscript: Kirby, Collier, Kharasch, Whittington, Thummel, and Unadkat.

Other: Collier and Kharasch oversaw and coordinated the conduct of the clinical studies.

References

Almond LM, Yang J, Jamei M, Tucker GT, and Rostami-Hodjegan A (2009) Towards a quantitative framework for the prediction of DDIs arising from cytochrome P450 induction. *Curr Drug Metab* **10:**420–432.

Bardsley-Elliot A and Plosker GL (2000) Nelfinavir: an update on its use in HIV infection. *Drugs* **59:**581–620.

Culm-Merdek KE, von Moltke LL, Gan L, Horan KA, Reynolds R, Harmatz JS, Court MH, and Greenblatt DJ (2006) Effect of extended exposure to grapefruit juice on cytochrome P450 3A activity in humans: comparison with ritonavir. *Clin Pharmacol Ther* **79:**243–254.

Dixit V, Hariparsad N, Li F, Desai P, Thummel KE, and Unadkat JD (2007) Cytochrome P450 enzymes and transporters induced by anti-human immunodeficiency virus protease inhibitors in human hepatocytes: implications for predicting clinical drug interactions. *Drug Metab Dispos* **35:**1853–1859.

Ernest CS 2nd, Hall SD, and Jones DR (2005) Mechanism-based inactivation of CYP3A by HIV protease inhibitors. *J Pharmacol Exp Ther* **312:**583–591.

Fahmi OA, Boldt S, Kish M, Obach RS, and Tremaine LM (2008a) Prediction of drug-drug interactions from in vitro induction data: application of the relative induction score approach using cryopreserved human hepatocytes. *Drug Metab Dispos* **36:**1971–1974.

Fahmi OA, Hurst S, Plowchalk D, Cook J, Guo F, Youdim K, Dickins M, Phipps A, Darekar A, Hyland R, et al. (2009) Comparison of different algorithms for predicting clinical drug-drug interactions, based on the use of CYP3A4 in vitro data: predictions of compounds as precipitants of interaction. *Drug Metab Dispos* **37:**1658–1666.

Fahmi OA, Maurer TS, Kish M, Cardenas E, Boldt S, and Nettleton D (2008b) A combined model for predicting CYP3A4 clinical net drug-drug interaction based on CYP3A4 inhibition, inactivation, and induction determined in vitro. *Drug Metab Dispos* **36:**1698–1708.

Greenblatt DJ, Peters DE, Oleson LE, Harmatz JS, MacNab MW, Berkowitz N, Zinny MA, and Court MH (2009) Inhibition of oral midazolam clearance by boosting doses of ritonavir, and by 4,4-dimethyl-benziso-(2*H*)-selenazine (ALT-2074), an experimental catalytic mimic of glutathione oxidase. *Br J Clin Pharmacol* **68:**920–927.

Greenblatt DJ, von Moltke LL, Harmatz JS, Chen G, Weemhoff JL, Jen C, Kelley CJ, LeDuc BW, and Zinny MA (2003) Time course of recovery of cytochrome p450 3A function after single doses of grapefruit juice. *Clin Pharmacol Ther* **74:**121–129.

Greenblatt DJ, von Moltke LL, Harmatz JS, Durol AL, Daily JP, Graf JA, Mertzanis P, Hoffman JL, and Shader RI (2000a) Alprazolam-ritonavir interaction: implications for product labeling. *Clin Pharmacol Ther* **67:**335–341.

Greenblatt DJ, von Moltke LL, Harmatz JS, Durol AL, Daily JP, Graf JA, Mertzanis P, Hoffman JL, and Shader RI (2000b) Differential impairment of triazolam and zolpidem clearance by ritonavir. *J Acquir Immune Defic Syndr* **24:**129–136.

Gupta A, Mugundu GM, Desai PB, Thummel KE, and Unadkat JD (2008) Intestinal human colon adenocarcinoma cell line LS180 is an excellent model to study pregnane X receptor, but not constitutive androstane receptor, mediated CYP3A4 and multidrug resistance transporter 1 induction: studies with anti-human immunodeficiency virus protease inhibitors. *Drug Metab Dispos* **36:**1172–1180.

Hsu A, Granneman GR, Witt G, Locke C, Denissen J, Molla A, Valdes J, Smith J, Erdman K, Lyons N, et al. (1997) Multiple-dose pharmacokinetics of ritonavir in human immunodeficiency virus-infected subjects. *Antimicrob Agents Chemother* **41:**898–905.

Hughes CA, Freitas A, and Miedzinski LJ (2007) Interaction between lopinavir/ritonavir and warfarin. *CMAJ* **177:**357–359.

Kharasch ED, Walker A, Hoffer C, and Sheffels P (2004) Intravenous and oral alfentanil as in vivo probes for hepatic and first-pass cytochrome P450 3A activity: noninvasive assessment by use of pupillary miosis. *Clin Pharmacol Ther* **76:**452–466.

Kirby B, Kharasch ED, Thummel KT, Narang VS, Hoffer CJ, and Unadkat JD (2006) Simultaneous measurement of in vivo P-glycoprotein and cytochrome P450 3A activities. *J Clin Pharmacol* **46:**1313–1319.

Kirby BJ and Unadkat JD (2010) Impact of ignoring extraction ratio when predicting drug-drug interactions, fraction metabolized, and intestinal first-pass contribution. *Drug Metab Dispos* **38:**1926–1933.

Koudriakova T, Iatsimirskaia E, Utkin I, Gangl E, Vouros P, Storozhuk E, Orza D, Marinina J, and Gerber N (1998) Metabolism of the human immunodeficiency virus protease inhibitors indinavir and ritonavir by human intestinal microsomes and expressed cytochrome P4503A4/3A5: mechanism-based inactivation of cytochrome P4503A by ritonavir. *Drug Metab Dispos* **26:**552–561.

Kumar GN, Rodrigues AD, Buko AM, and Denissen JF (1996) Cytochrome P450-mediated metabolism of the HIV-1 protease inhibitor ritonavir (ABT-538) in human liver microsomes. *J Pharmacol Exp Ther* **277:**423–431.

Lillibridge JH, Liang BH, Kerr BM, Webber S, Quart B, Shetty BV, and Lee CA (1998) Characterization of the selectivity and mechanism of human cytochrome P450 inhibition by the human immunodeficiency virus-protease inhibitor nelfinavir mesylate. *Drug Metab Dispos* **26:**609–616.

Obach RS, Walsky RL, and Venkatakrishnan K (2007) Mechanism-based inactivation of human cytochrome P450 enzymes and the prediction of drug-drug interactions. *Drug Metab Dispos* **35:**246–255.

Ripp SL, Mills JB, Fahmi OA, Trevena KA, Liras JL, Maurer TS, and de Morais SM (2006) Use of immortalized human hepatocytes to predict the magnitude of clinical drug-drug interactions caused by CYP3A4 induction. *Drug Metab Dispos* **34:**1742–1748.

Thummel KE, O'Shea D, Paine MF, Shen DD, Kunze KL, Perkins JD, and Wilkinson GR (1996) Oral first-pass elimination of midazolam involves both gastrointestinal and hepatic CYP3A-mediated metabolism. *Clin Pharmacol Ther* **59:**491–502.

Tran TH, Von Moltke LL, Venkatakrishnan K, Granda BW, Gibbs MA, Obach RS, Harmatz JS, and Greenblatt DJ (2002) Microsomal protein concentration modifies the apparent inhibitory potency of CYP3A inhibitors. *Drug Metab Dispos* **30:**1441–1445.

Wang Z, Gorski JC, Hamman MA, Huang SM, Lesko LJ, and Hall SD (2001) The effects of St John's wort (*Hypericum perforatum*) on human cytochrome P450 activity. *Clin Pharmacol Ther* **70:**317–326.

Zeldin RK and Petruschke RA (2004) Pharmacological and therapeutic properties of ritonavir-boosted protease inhibitor therapy in HIV-infected patients. *J Antimicrob Chemother* **53:**4–9.

Zhao P (2008) The use of hepatocytes in evaluating time-dependent inactivation of P450 in vivo. *Expert Opin Drug Metab Toxicol* **4:**151–164.

Address correspondence to: Dr. Jashvant D. Unadkat, Department of Pharmaceutics, School of Pharmacy, Box 357610, University of Washington, Seattle WA 98195-7610. E-mail: jash@u.washington.edu